

In-plane current-voltage characteristics and oscillatory Josephson-vortex flow resistance in La-free $\text{Bi}_{2+x}\text{Sr}_{2-x}\text{CuO}_{6+\delta}$ single crystals in high magnetic fields

S. I. Vedenev^{1,2} and D. K. Maude¹

¹ Grenoble High Magnetic Field Laboratory, Centre National de la Recherche Scientifique, B.P. 166, F-38042 Grenoble Cedex 9, France

² P.N. Lebedev Physical Institute, Russian Academy of Sciences, 119991 Moscow, Russia

(Dated: November 13, 2018)

We have investigated the in-plane $I(V)$ characteristics and the Josephson vortex flow resistance in high-quality La-free $\text{Bi}_{2+x}\text{Sr}_{2-x}\text{CuO}_{6+\delta}$ (Bi2201) single crystals in parallel and tilted magnetic fields at temperatures down to 40 mK. For parallel magnetic fields below the resistive upper critical field H_{c2}^* , the $I(V)$ characteristics obey a power-law with a smooth change with increasing magnetic-field of the exponent from above 5 down to 1. In contrast to the double-layer cuprate Bi2212, the observed smooth change suggests that there is no change in the mechanism of dissipation (no Kosterlitz-Thouless transition) over the range of temperatures investigated. At small angles between the applied field and the ab -plane, prominent current steps in the $I(V)$ characteristics and periodic oscillations of Josephson-vortex flow resistance are observed. While the current steps are periodic in the voltage at constant fields, the voltage position of the steps, together with the flux-flow voltage, increases nonlinearly with magnetic field. The ab -flow resistance oscillates as a function of field with a constant period over a wide range of magnetic fields and temperatures. The current steps in the $I(V)$ characteristics and the flow resistance oscillations can be linked to the motion of Josephson vortices across layers.

PACS numbers: 74.72.Hs, 74.60.Ec, 74.25.Ey

I. INTRODUCTION

It is now well established that the stack of Josephson junctions formed by the atomic layers of high-temperature superconductors (HTSC) represents a non-linear system with unique dynamic properties. A magnetic field perpendicular to the layers induces Abrikosov-type pancake vortices in the planes. In contrast, a magnetic field applied along the CuO_2 layers (parallel to the ab -planes) creates Josephson vortices, each carrying one flux quantum, and whose cores are located between the superconducting layers. When the parallel magnetic field exceeds the crossover field, $H_{cr} = \Phi_0/\pi\gamma s^2$, where Φ_0 is the flux quanta, γ is the anisotropy of the London penetration depth, and s is the interlayer spacing, the cores of Josephson vortices start to overlap and a Josephson lattice is formed.¹ At the same time, the vortex ground state and the vortex phase diagram of highly-anisotropic (layered) HTSC in parallel and oblique magnetic fields remains the open question. The picture of a phase transition from a solid (phase-ordered) state to a liquid state of a combined lattice structure of Josephson vortices and pancake vortices in high magnetic fields also remains unclear.²

Due to the proximity to the Mott insulator, phase fluctuations are strong and the temperature of the superconducting transition, T_c , in cuprates may be governed by phase fluctuations. In two dimensions, the phase fluctuations can give rise to a Kosterlitz-Thouless transition which is described by the thermal unbinding of vortex-antivortex pairs. However, there is no clear picture for the destruction of superconducting order in layered HTSC via the unbinding of vortices.³ Emery

and Kivelson⁴ have calculated the Kosterlitz-Thouless transition in layered HTSC assuming that each layer is fluctuating independently, even for systems with strongly Josephson coupled bilayers. On the other hand, Corson *et al.*⁵ using microwave conductivity have confirmed the Kosterlitz-Thouless nature of the phase transition but concluded that in $\text{Bi}_2\text{Sr}_2\text{CaCu}_2\text{O}_{8+\delta}$ (Bi2212) system it is the bilayer which should be considered as a unit, i.e., the superconducting phase is strongly correlated between the two layers of a bilayer. In view of these findings, it is interesting to look for a Kosterlitz-Thouless transition in the single-layer high- T_c superconductor $\text{Bi}_2\text{Sr}_2\text{CuO}_{6+\delta}$ where the interlayer spacing is considerable more. As previously reported,^{6,7,8} this can be achieved by measuring the $I(V)$ characteristics of the samples. Bi2212 single crystals, both in zero and in applied magnetic fields, show non-ohmic, power-law $I(V)$ characteristics. The observed power-law behavior, $V \sim I^{\alpha(T,H)}$, with a characteristic jump in the exponent $\alpha(T,H)$ near the superconducting transition has been interpreted as evidence for the Kosterlitz-Thouless transition.

It is apparent that to gain a better understanding of the vortex ground state and vortex phase diagram in HTSC, it is essential to understand the dynamics of Josephson vortices. In the generally studied geometry, a c -axis external current drives Josephson vortices in the direction perpendicular to both the current and the magnetic field. The driven motion of the vortices is responsible for the observed flow resistance. Koshelev⁹ calculated the flux-flow resistivity of the Josephson vortex lattice in a layered superconductor and showed that the magnetic field dependence of the flux-flow resistivity is characterized by three distinct regions. At low magnetic fields

the flux-flow resistivity grows linearly with field. When the Josephson vortices start to overlap the flux-flow resistivity crosses over to a regime of quadratic magnetic field dependence. Finally, at very high fields the flux-flow resistivity saturates at a value close to the c -axis quasiparticle resistivity.

A Josephson lattice driven by a current along the c axis, together with the resulting flux-flow resistance, has been intensively studied both experimentally and theoretically because the coherent Josephson vortices motion gives rise to strong resonant phenomena which may lead to very important applications of high- T_c superconductors.¹⁰ In particular, the flux-flow voltage creates an oscillating current through the Josephson effect and the current excites Josephson plasma waves at Terahertz frequency. Part of the energy may be emitted as electromagnetic waves.¹¹ Under appropriate conditions, coherent motion of Josephson vortices is possible and this can excite cavity resonances of the stack (the Fiske resonances), which in turn influence the vortex motion. Such geometric resonances manifest themselves in the c -axis current voltage ($I(V)$) characteristic as a series of steps separated by a constant voltage.^{12,13} Recently, Ooi *et al.*¹⁴ reported novel periodic oscillations of the flux-flow resistance with a c -axis bias current. The measured periodicity, H_p , is given by the relation $\Phi_0/2ws$ where w is the sample size in the ab -plane along the direction perpendicular to the applied magnetic field. Such oscillations of the Josephson vortices flow resistance can be explained by a matching effect between the lattice spacing of Josephson vortices along the layers and the size of the sample.

It should be noted that in Josephson-coupled layered superconductors, vortices exist for any orientation of the magnetic field. In the presence of an electrical current, the Lorentz force on vortices causes motion which generates both in-plane and interplane electric fields and which induces a flux-flow voltage drop across the superconducting sample. The sliding motion of Josephson vortices along the ab -plane is easily driven by a current along the c axis. For a driving force exerted along the c axis (current in the ab -plane), the CuO_2 planes effectively pin the Josephson vortices preventing motion along the c axis.¹⁵ The dynamics of the Josephson lattice along the c axis is far from being fully understood. In tilted high fields $H \gg H_{cr}$ at small angles between the applied field and the ab -plane, a zigzag structure along the c axis arising from the attractive interaction of pancake vortices with Josephson vortices, see Ref. [16]. In this case one might expect a series of maxima in the plasma frequency and the critical current at angles for which the pancake lattice is in resonance with the Josephson lattice.

Investigations of the dynamics of the vortex lattice in HTSC are usually limited to the region near T_c because the large critical current density J_c makes low-temperature studies difficult, whereas in clean systems the vortex lattice is expected to melt due to thermal fluctuations. Values of the upper critical field H_{c2} and J_c in

the $\text{Bi}_2\text{Sr}_2\text{CuO}_{6+\delta}$ system are relatively low, which allows to observe the effect of strong magnetic fields on the dynamics of the Josephson vortex lattice at very low temperatures below and above a melting line where the magnetic field behavior depends on the mechanism of dissipation.

Here, we present an experimental study of the in-plane $I(V)$ characteristics and the in-plane Josephson vortex flow resistance in parallel and tilted magnetic fields in single-layer La-free $\text{Bi}_2\text{Sr}_2\text{CuO}_{6+\delta}$ single crystals at temperatures down to 40 mK. At small angles θ between the applied field and ab -plane, we have found prominent current steps in the $I(V)$ characteristics and periodic oscillations in the Josephson-vortex flow resistance. To gain a better understanding as to the nature of the observed current steps and periodic oscillations, we have compared the behavior of the in-plane flux flow resistance in Bi2201 single crystals with the published data for Bi2212 with double CuO_2 layers.

II. EXPERIMENT

The high-quality La-free $\text{Bi}_{2+x}\text{Sr}_{2-x}\text{CuO}_{6+\delta}$ (Bi2201) single crystals used for the present study were grown by a KCl-solution-melt free growth method.^{17,18} The preparation and characterization of Bi2201 single crystals are described in detail elsewhere.¹⁹ As before, in this work we have used *as-grown* single crystals. The properties of the samples investigated in this work are summarized in Table I. The temperature dependence of the resistance of the present samples in zero magnetic field are essentially the same as those we reported previously.¹⁹ We have measured the resistance, $I(V)$ characteristics and the differential resistance $dV/dI(V)$ characteristics for Bi2201 single crystals using a standard four-probe technique with symmetrical positions of the low-resistance contacts on both ab surfaces of the sample.²⁰ The current was applied parallel to the ab -plane in all cases. In the experimental arrangement used, the crystal could be rotated *in-situ* relative to the direction of the magnetic field with an angular resolution better than 0.1° . The $\theta = 0^\circ$ orientation was precisely determined from the lowest value of the resistance at a fixed temperature. A configuration with $H \perp J$ was used always. Measurement procedures in the resistive magnet are described in detail in Refs. [19,21].

TABLE I: Doping (p), critical temperature (T_c) determined from the 50% point of the resistive transition, and dimensions for the Bi2201 single crystals investigated. Optimal doping in Bi2201 occurs at $p \simeq 0.17$ holes per Cu.

Sample	p (holes/Cu)	T_c (K)	Size ($l \times w \times d$)
#5	0.17	9.8	1.8 mm \times 0.7 mm \times 2 μm
#7	0.14	5.5	1.5 mm \times 0.7 mm \times 1 μm
#4	0.13	3.6	3 mm \times 0.3 mm \times 1 μm
#2	0.12	2.0	1 mm \times 0.75 mm \times 1 μm

III. RESULTS AND DISCUSSION

A. Current-voltage characteristics

As reported in Ref. [7], a parallel external magnetic field plays a crucial role in the dynamics of the Kosterlitz-Thouless transition, and in particular, reduces the transition temperature. In sufficiently strong magnetic fields parallel to the ab -plane (up to 8 T), the Kosterlitz-Thouless transition is suppressed because the magnetic field-induced vortices increase the dissipation and reduces the stability of the vortex-antivortex pairs. However, subsequently, it has been suggested²² that in Bi2212 at high parallel magnetic fields, there is a multi-critical point in the H - T phase diagram characterized by a magnetic field $H_{mc} = \Phi_0/2\sqrt{3}\gamma s^2$, above which exists a novel intermediate Kosterlitz-Thouless type phase. The existence of this intermediate phase was also confirmed by the non-ohmic power-law $I(V)$ characteristics in the Bi2212 system. Chen and Hu²³ very recently investigated theoretically the in-plane $I(V)$ characteristics of inter-layer Josephson vortices in cuprate HTSC using a computer simulation and showed that for highly anisotropic systems ($\gamma = 20$) and at high magnetic field, the power-law in-plane $I(V)$ characteristics changes its exponent from 1 (i.e., Ohmic) at high temperatures to ≥ 3 at intermediate temperatures, which can be attributed to a Kosterlitz-Thouless transition.

In layered high- T_c superconductors, the anisotropy is usually expressed by the ratio $\gamma = \lambda_c/\lambda_{ab}$, where λ_c is the London penetration depth for super currents along the c axis, and λ_{ab} is the penetration depth for currents in the ab -plane. The anisotropy ratio γ can also be expressed by the ratio $\sqrt{m_c/m_{ab}}$ between the effective masses of the quasiparticles along the c -axis and in the ab -plane, which can be related to the transport anisotropy with $\gamma \simeq \sqrt{\rho_c/\rho_{ab}}$ using $\rho = m/ne^2\tau$ for the out-of-plane resistivity ρ_c and in-plane resistivity ρ_{ab} .^{24,25,26}

Owing to the large value of H_{c2} in parallel magnetic fields, in order to study the power-law behavior of the $I(V)$ characteristics of Bi2201 single crystals, we have used underdoped samples with a low T_c . Previously, we found¹⁹ that the normal-state anisotropy ratio ρ_c/ρ_{ab} in high magnetic fields and at low temperatures is practically temperature independent. For this reason, we can safely neglect any variation of γ for the temperatures used here. For the underdoped #7 ($T_c = 5.5$ K) and heavily underdoped #2 ($T_c = 2$ K) samples, the anisotropy is equal to $\gamma \simeq 40$ and $\gamma \simeq 22$, respectively. In this case the values of the multi-critical magnetic field H_{mc} should be $\simeq 10$ T and $\simeq 18$ T.

The in-plane current-voltage characteristics for samples #7 and #2 near the magnetic-field induced suppression of superconductivity at 0.6 K and 40 mK are plotted using a logarithmic scale in Fig. 1(a) and Fig. 1(b), for selected magnetic fields ($H \parallel ab$). The temperature dependence of the resistance $R_{ab}(T)$ of the present samples in zero magnetic field (not shown) are essentially the

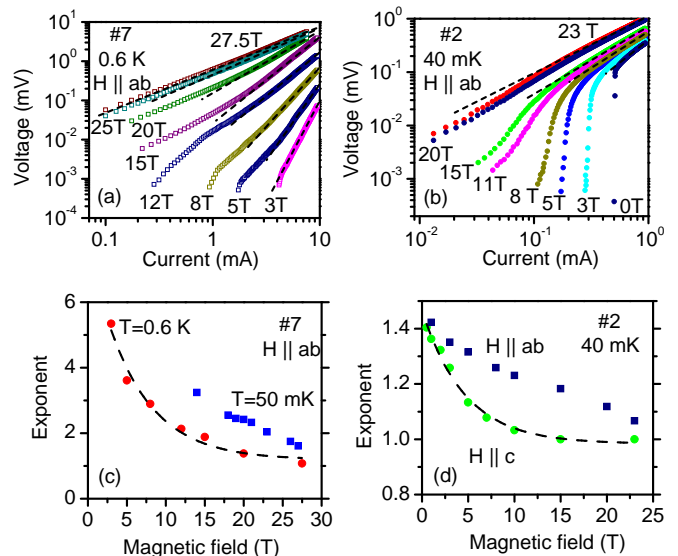


FIG. 1: (color on-line) (a) $I(V)$ characteristics plotted using a logarithmic scale for samples #7 (a) and #2 (b) near the magnetic-field induced suppression of the superconductivity at 0.6 K and 40 mK for selected magnetic fields oriented parallel to the ab -plane. The dashed lines are power-law fits to the data. (c) and (d) Magnetic-field dependence of the power-law exponent for samples #7 and #2, respectively.

same as those reported previously for samples with the same doping.¹⁹

The $I(V)$ characteristics can be fitted to a power law for currents above a critical current I_c (dashed lines in Fig.1(a-b)). The extracted power law exponent, α , of the $I(V)$ characteristics, is plotted in Figures 1(c) and 1(d) as a function of magnetic field for samples #7 and #2, respectively, at 0.6 K, 50 mK and 40 mK. At $T = 0.6$ K, α decreases rapidly with increasing field and its value tends to unity in high magnetic fields, while at very low temperature, α decreases much more slowly. However, although the $I(V)$ characteristics show a power-law behavior with the change in the value of exponent from 1 to above 5 [Fig. 1(c)] and the magnetic fields far exceed the H_{mc} value, both the figures show that α decreases smoothly with increasing field, without any features that might be interpreted as evidence for a transition to the Kosterlitz-Thouless type phase. It should be noted that the magnetic fields 23 T and 28 T applied here are far in excess of the fields at which the 3D vortex melting occurs in low T_c Bi2201 samples.²⁷

It has been suggested in Refs. [6,28], that the power law dependence of the $I(V)$ curves at low temperatures is related to the interplay of the in-plane vortex lines and the two-dimension pancake vortices created by a small component of the magnetic field parallel to the c axis. That can appear because of a small misalignment to the c axis within the crystal. However, we also observe a power-law behavior in the ab -plane $I(V)$ characteristics when the magnetic field is applied perpendicular to ab -plane. In Fig. 1(d), we also plot the power-law exponent

versus magnetic field applied along the c -axis for crystal #2 at $T = 40$ mK. One can see that α lies in the same range for both orientations of the field. In view of this, it is difficult to imagine that a possible small c -axis component of the magnetic field (in the parallel geometry) gives the same change in the value of α as the large magnetic field oriented along the c -axis. In addition, we can formally exclude macroscopic sample inhomogeneity, as the origin of the observed the power-law behavior in $I(V)$ characteristics in Fig. 1(a) and Fig. 1(b), the crystals are of a very high quality judging from the small rocking curve width $\leq 0.1^\circ$.

B. Differential resistance

In high magnetic fields, the in-plane $I(V)$ characteristics in low bias region (small currents) showed unusual behavior for a superconductor. This feature in the $I(V)$ characteristic in the vicinity of the zero bias can be more clearly seen the measured first derivatives $dV/dI(V)$ for the sample #2 with current and voltage contacts on the same surface of the crystal at a temperature of $T = 40$ mK with the magnetic field oriented perpendicular and parallel to the ab -plane.

In Fig. 2(a) (main panel), we plot the voltage dependence of the differential resistance $dV/dI(V)$ near the current induced suppression of the superconductivity in different magnetic fields applied along the c -axis of the crystal #2 at $T = 40$ mK. In the inset, we plot the the magnetoresistance $R_{ab}(H)$ measured at $T = 40$ mK for the same sample with the magnetic field applied along the c -axis. As can be seen, the differential resistance $dV/dI(V)$ saturates at high fields in accordance with the exponent $\alpha(H)$ in Fig. 1(c) and Fig. 1(d). The $dV/dI(V)$ curves have a minimum close to zero bias voltage, the amplitude of which decreases with increasing magnetic field. This minima should disappear at a magnetic field corresponding to the transition of the sample to the normal state. What is observed is slightly different since this minimum transforms to a maximum for magnetic fields ≥ 15 T after the suppression of the superconductivity (marked by arrows in the inset and main panel). It can be supposed that such a behavior of the differential resistance in the vicinity of low bias at magnetic fields above the resistive upper critical field H_{c2}^* is connected with moving vortex-like excitations which have been previously observed in superconducting cuprates at $T > T_c$ in magnetic fields by the detection of a Nernst signal²⁹ and measurement of an angular dependence of the magnetoresistance on $Y_{1-x}Pr_xBa_2Cu_3O_{7-\delta}$ single crystals.³⁰ With increasing current, the number of vortices decreases and the differential resistance in Fig. 2(a) decreases rapidly.

Figure 2(b) (main panel) shows the analogous $dV/dI(V)$ curves for the same sample in the magnetic fields applied in the ab -plane of the crystal at $T = 40$ mK. For clarity, the curves have been shifted vertically with respect to the upper curve. In the inset we show the

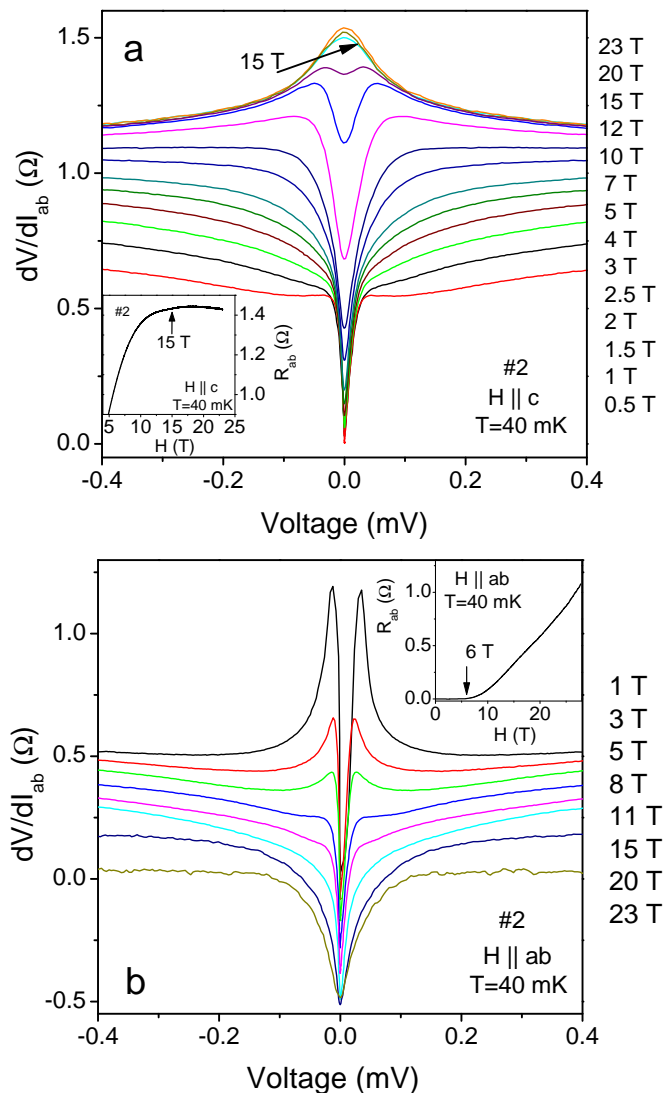


FIG. 2: (color on-line) Differential resistance $dV/dI(V)$ near the current induced suppression of superconductivity at $T = 40$ mK for different magnetic fields applied along the c -axis of the crystal #2 (a) and along ab -plane (b). For clarity, the curves in (b) have been shifted vertically (downwards) with respect to the upper curve. The inset in (a) shows the magnetoresistance $R_{ab}(H)$ measured at $T = 40$ mK for the sample #2 with the magnetic field applied along the c -axis. The inset in (b) shows the magnetoresistance $R_{ab}(H)$ measured at $T = 40$ mK for the sample #2 in a parallel magnetic field ($H \parallel ab$).

magnetoresistance $R_{ab}(H)$ measured at $T = 40$ mK for the same sample in a parallel magnetic field (the onset of the superconducting transition is marked by an arrow). Despite the different types of vortex lattice (the pancake vortices in perpendicular and Josephson vortices in parallel configurations), the $dV/dI(V)$ curves in Fig. 2(b) have a general form identical to that in Fig. 2(a). At our maximum field $H = 28$ T, the resistance of the sample has only reached 70% of its normal-state value and

the minimum of the differential resistance in the vicinity of low bias currents is not completely suppressed. This suggests that the mechanism of the dissipation in the neighborhood of H_{c2}^* is common to both magnetic field directions.

These results allows us to conclude that the behavior of the flux flow resistance in the ab -plane in Bi2201 single crystals at low temperatures is largely similar to that in Bi2212 except for the absence of a transition to the Kosterlitz-Thouless phase. Apparently, this transition does not take place at low temperatures even in high magnetic fields. Most likely the Kosterlitz-Thouless transition in Bi2201 can be observed only in a very narrow temperature region near T_c .

C. Current steps in $I(V)$ characteristics

The interaction of the pancake vortices with the Josephson vortices can lead to features in the $I(V)$ characteristics with the transport current along the ab -plane when the period of the pancake vortex lattice matches the period of the Josephson vortex lattice. In order to rule out the presence of spatial inhomogeneity, which can be present in underdoped samples and which may influence the results found, we have used for these measurements an optimally doped Bi2201 single crystal (#5) with $T_c = 9.8$ K. To investigate the influence of misalignment between the magnetic field and the superconducting layers, the sample was rotated at small angles around its position of parallel to the layers. Temperatures for these measurements were chosen so that the available magnetic field would suffice to observe the flux-flow voltage while remaining below the melting line. With increasing current in the ab -plane, we have found prominent current steps in the $I(V)$ characteristics. The amplitude of the current steps depends on the angle between the applied field and the ab -plane. At very small angles θ , as in the parallel configuration of field, no current steps are observed in the $I(V)$ characteristics. This is consistent with the sample remaining free of pancake vortices until the normal component $H \sin \theta$ exceeds the perpendicular critical field H_{c1} for pancake formation.³¹ For a detailed investigation, we chose the orientation of the field for which the amplitude of the current steps was a maximum.

Figure 3(a) (main panel) displays the $I(V)$ characteristics for the single crystal #5 in various tilted magnetic fields at 0.8 K with transport current flowing in the ab -plane perpendicular to the applied magnetic field. Current steps are clearly observed (for $H = 23$ T, they are marked by arrows). The angle θ between the applied field and the ab -plane was equal to 4° . The inset in Fig. 3(a) shows similar characteristics for two different magnetic fields at $\theta = 2^\circ$.

In Fig. 3(b) (main panel), we plot the voltage position of the current steps versus magnetic field (the number of the current step are indicated for each curve). It can

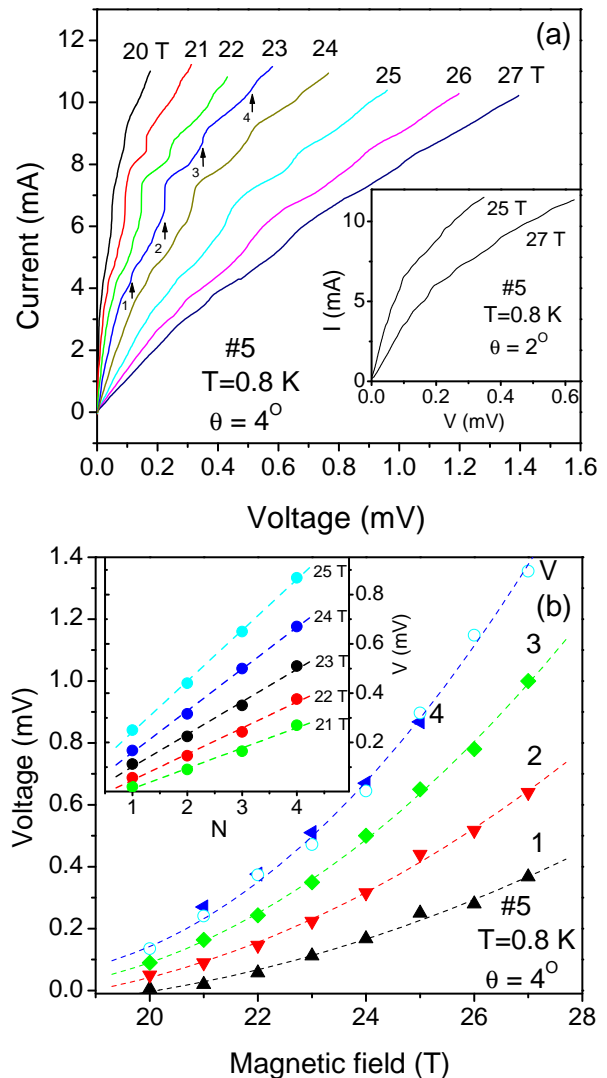


FIG. 3: (color on-line) (a) $I(V)$ characteristics of sample #5 with $T_c = 9.8$ K in various tilted ($\theta = 4^\circ$) magnetic fields at 0.8 K with the transport current flowing in the ab -plane perpendicular to the field. Current steps are indicated by arrows. The inset in Fig. 3(a) shows similar characteristics for two different magnetic fields at $\theta = 2^\circ$. (b) Voltage position of the current steps versus magnetic field (solid symbols). The number of the current step is indicated for each curve. Open circles show the flux-flow voltage for a current of 10 mA. The dashed lines are fits to the experimental data. The inset shows the voltage position of the current steps versus the step number for different fields.

be seen that the voltage position of each step increases nonlinearly with magnetic field (solid symbols) as well as the flux-flow voltage, at the current 10 mA showed by open circles. It is evident that the data can be fitted quite well to curves of the form $V = aH + bH^2$ where a and b are constants (dashed lines).

These steps cannot be attributed to Fiske steps caused by an interaction of the ac Josephson effect with electromagnetic modes of a cavity formed by the Josephson

junctions (geometric resonance) for a number of reasons. Firstly, the dc voltage is applied along the ab -plane instead of across the junctions and secondly, the voltage position of the current steps depends on the magnetic field which is not expected for Fiske resonances. Furthermore, while the current steps are periodic in the voltage at constant fields, the step period increases with increasing magnetic field. This can be seen in the inset of Fig. 3(b) where we show the voltage position of the current steps versus the step number for different fields.

On the other hand, the range of the magnetic fields in Fig. 3(a) at $\theta = 4^\circ$ exceeds the crossover field H_{cr} for sample #5 and also the field component perpendicular to the layers exceeds the perpendicular lower critical field H_{c1} for pancake formation. Under these conditions, according to the model of Bulaevskii *et al.*¹⁶, the tilted magnetic field induces a triangular lattice of Josephson vortices and pancake vortices which form a zigzag structure along the c axis. In this case one might expect a series of maxima in the c -axis plasma frequency and the c -axis critical current at angles where the pancake lattice is in resonance with the Josephson lattice. Such zigzag structure result in oscillations of the out-of-plane resistance and a sharp increase of the c -axis critical current in Bi2212 single crystal at 30 K in field 20 T at small angles near $\theta = 0^\circ$ with width $\approx 2^\circ$.¹⁶ Based on the model of Bulaevskii *et al.*¹⁶, we estimate that the periods of the Josephson and pancake lattices in our experiment, for example, at $H = 23$ T should be matched at $\theta \simeq 1^\circ$. This is in disagreement with the observed maximum amplitude of the current steps at $\theta \simeq 4^\circ$. We do not understand the reason for this discrepancy. However, subsequent studies^{32,33} after Ref. [16] have shown that the maximum of such resonance in Bi2212 single crystals at $T = 5$ K takes place at the angle $\theta = 5^\circ$ and the angular dependence of the resonance field is much more drastic than the result of Ref. [16].

In our case, with the magnetic field component parallel to the layers and the current flowing in the ab -plane, the Lorentz force acting on the vortices drives them parallel to the c axis with jumps across the superconducting layers. The motion of the Josephson lattice generates both in-plane and out-of-plane alternating electric fields and currents, which are coupled to electromagnetic plasma waves. There should exist a strong resonance emission when the velocity of the lattice matches the velocity of the plasma wave.³⁴ The matching of the Josephson frequency with the frequency of the emission may manifest itself as the current steps not only in the c -axis current, but possibly in the in-plane current as well [Fig. 3(a)]. Since the behavior of the plasma mode in parallel and tilted fields is poorly understood at present, in contrast to the perpendicular magnetic field geometry, we are unable to discuss here this topic more fully. However, since it was assumed that the periodic steps in the in-plane $I(V)$ characteristics may be related to the moving Josephson vortex lattice along the c axis, we have tried to experimentally establish this fact.

D. Flow resistance oscillations

As noted above, Ooi *et al.*¹⁴ found periodic oscillations of the c -axis flow resistance of Josephson vortices as a function of the in-plane magnetic field in small-strip Bi2212 single crystal in a wide range of temperatures and fields. A resistance of the strip sample in used geometry was almost equal to the c -axis resistance of the intrinsic junctions and the contribution of in-plane resistivity was neglected. These oscillations were related to a matching effect between the lattice spacing of Josephson vortices along the layers and the width of the sample. Subsequently, Koshelev³⁴ and Machida¹⁵ have reproduced the oscillation by calculating the flux flow resistance by taking the surface barrier effect into consideration.

An attempt to observe the periodic oscillations of the ab -plane flow resistance of Josephson vortices in a parallel magnetic field similar to Ref. [14] in our crystal with usual sizes¹⁹ has been unsuccessful. Because of this, we have measured the in-plane Josephson vortex flow resistance versus parallel and tilted magnetic fields in a Bi2201 strip single crystal #4 with $T_c = 3.6$ K. In spite of the low T_c , a careful characterization of the crystal showed the high quality, the high homogeneity and the structural perfection of the sample. As the magnetic field was oriented parallel to the ab -planes exactly, the ab -flow resistance increased smoothly with increasing field because only the number of vortices increased. At the same time, the resistance begins to oscillate as a function of the magnetic field for any small deviation of the field from the exactly parallel geometry as shown by three curves in Fig. 4. The amplitude of oscillations gradually diminishes with increasing magnetic field and oscillations are not observed at fields above 15 T. The oscillations also rapidly vanish when the angle θ between the applied field and the ab -plane exceeded $\approx 6^\circ$. The maximum amplitude of the oscillations was reached at $\theta \approx 4^\circ$. At the same time, the oscillations are most prominent at higher temperatures where thermal fluctuations reduce the role of background pinning and the crystal behaves as if it contains fewer defects than it actually does.

It can be seen from the inset in Fig. 4 that the period of the oscillations $\Delta H \approx 1.9$ T is to a good approximation constant over a wide range of magnetic fields. The period also does not depend on the temperature (see curves for three different temperatures in Fig. 4). The oscillations can be observed for almost all temperatures below T_c , but have reduced amplitude at very low temperatures and near T_c .

The flow resistance oscillations in Fig. 4 are quite similar to the oscillations of the c -axis Josephson-vortex flow resistance in Bi2212 single crystals previously observed by Ooi *et al.*¹⁴. The oscillations in Ref.[14] originate from a matching between the triangular lattice and the width w of the junction perpendicular to the magnetic field direction. The period of the oscillations, H_p , corresponded to adding one flux quantum Φ_0 per two layers in the crystalline lattice. The minima in the resistance

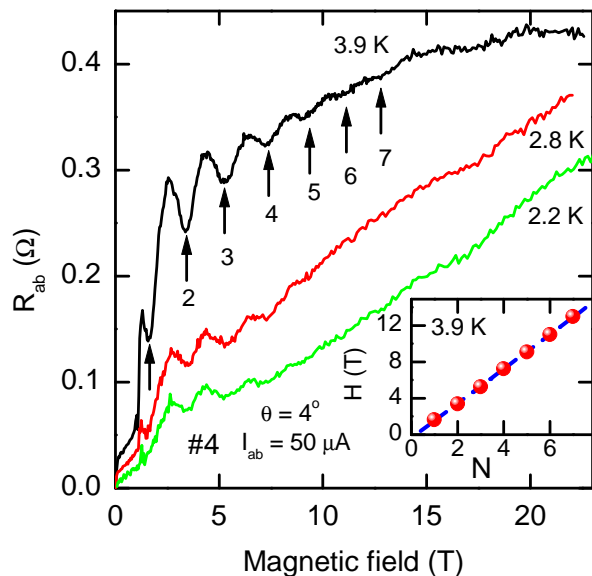


FIG. 4: (color on-line) Flow resistance of the Josephson vortices as a function of magnetic field for sample #4 with an applied current of $50\mu\text{A}$ at different temperatures. The inset shows the magnetic field position of the resistance minima (marked by arrows in the main panel) versus the number ($N = 1$ corresponds to the minima closest to zero bias) at $T = 3.9$ K.

corresponded to the condition where the magnetic field was $nH_p \approx nH_0/2$ (n is an integer). Here $H_0 = \Phi_0/ws$ is the field needed to add one vortex per layer in a Bi2212, where s is the periodicity of the CuO_2 double layers.

In Ref. [14], a transport current flowing across the layers exerts a Lorentz force on the Josephson vortices in the plane of layers. An important parameter is the critical current above which the lattice starts to move, producing a finite voltage. This current is determined either by bulk pinning or by interaction with the boundaries.³⁵

For the measured flow resistance in Fig. 4, a transport current flowing along the layers increases the effect of the Lorentz force on the Josephson vortices across the layers. Due to the interaction with the boundaries of the sample, the period of oscillations in Fig. 4 should depend on the size of the sample along the c -axis direction. The flow resistance shows periodic oscillations with period $\Delta H \approx 1.9$ T which is very close (within the accuracy of measuring the sample thickness) to the estimated $H_0 = \Phi/ds = 1.7$ T, corresponding to the magnetic field needed to add one vortex quantum per layer in the crystalline lattice. Here d is the size of our strip single crystal along c axis (thickness) and $s = 12.3$ Å is the distance between the superconducting CuO_2 layers in Bi2201. This result suggests that Josephson vortices in Bi2201 form a square lattice in the ground state. As before, the oscillations are most prominent in the high temperature regime where thermal fluctuations reduce the role of background pinning and the crystal behaves as if it contained fewer defects than it actually does.

We note that somewhat similar commensurate oscillations of the ab -plane resistivity for magnetic fields nearly aligned with the ab -plane has been observed on $\text{YBa}_2\text{Cu}_3\text{O}_{7-\delta}$ single crystals in earlier work by Gordeev *et al.*³⁶. These oscillations are due to the oscillatory melting line separating the vortex liquid from the vortex smectic state and they are periodic in $H^{-1/2}$. This is very different from the periodic in H oscillations of the vortex-flow resistance reported in Ref.[14] and observed here, which in addition are observed over a wide range of temperatures and magnetic fields below and above a melting line.

E. Discussion

Finally, it is pertinent to recall here a transport phenomenon which has its origins in a Lorentz-force-independent dissipation that has been observed in strongly coupled layered Bi- and Tl-based materials.^{6,7,8,37} For this case the resistivity in the non-Ohmic regime did not depend on the angle between the magnetic field and current when they are both parallel to the layers. The problem of an orientation-independent dissipation and the role of the Lorentz force in the motion of the Josephson vortex lattice cannot be explained by simple flux-flow theory and is far from being totally understood.

Turning back to Fig. 3(a), we can suppose that the motion of the Josephson lattice generates a traveling electromagnetic wave with the ab -plane wave vector selected by the lattice structure. One might expect resonance phenomena when the velocity of the lattice matches the plasma wave velocity.³⁴ On the other hand, if the motion of the Josephson vortex lattice generates a voltage across the layers, one would expect that the current steps in Fig. 3(a) are due to the matching of the Josephson frequency with the frequency of the plasma mode. Both mechanisms may result in the current steps in the $I(V)$ characteristics.

IV. CONCLUSION

In summary, we have studied the in-plane $I(V)$ characteristics and Josephson vortex flow resistance in La-free Bi2201 single crystals in parallel and tilted magnetic fields at temperatures down to 40 mK. For parallel magnetic fields, we find a power-law $I(V)$ characteristic with a smooth decrease with magnetic-field of the exponent describing the power-law. At small angles between the applied field and ab -plane, prominent current steps in the $I(V)$ characteristics and periodic oscillations of Josephson-vortex flow resistance are observed. While the current steps are periodic in the voltage at constant fields, the voltage position of the steps, together with the flux-flow voltage, increases nonlinearly with increasing magnetic field. The ab -flow resistance oscillates as

a function of magnetic field with a constant period over a wide range of magnetic fields and temperatures. The current steps in the $I(V)$ characteristics and the flow resistance oscillations can be linked to the motion of the Josephson vortices across layers.

Acknowledgments

This work has been partially supported by PICS grant No. 3447. One of us (S.I.V.) was partially supported by

the Russian Foundation for Basic Research Projects No. 06-02-22001 and No. 07-02-00349. The work at GHMFL was partially supported by the European 6th Framework Program under contract number RITA-CT-3003-505474.

-
- ¹ L. N. Bulaevskii, Sov. Phys. JETP **37**, 1133 (1973).
² M. Konczykowski, C. J. van der Beek, A. E. Koshelev, V. Mosser, M. Dodgson, and P. H. Kes, Phys. Rev. Lett. **97**, 237005 (2006), and references therein.
³ P. A. Lee, Rev. Mod. Phys. **78**, 17 (2006).
⁴ V. J. Emery and S. Kivelson, Nature (London) **374**, 434 (1995).
⁵ J. Corson, R. Mallozzi, J. Orenstein, J. Eckstein, and I. Bozovic, Nature (London) **398**, 221 (1999).
⁶ Y. Ando, N. Motohira, K. Kitazawa, J. I. Takeya, and S. Akita, Phys. Rev. Lett. **67**, 2737 (1991).
⁷ A. K. Pradhan, S. J. Hazell, J. W. Hodby, C. Chen, Y. Hu, and B. M. Wanklyn, Phys. Rev. B **47**, 11374 (1993).
⁸ Y. Iye, S. Nakamura, and T. Tamegai, Physica C **159**, 433 (1989).
⁹ A. E. Koshelev, Phys. Rev. B **62**, R3616 (2000).
¹⁰ B. Y. Zhu, H. B. Wang, S. M. Kim, S. Urayama, T. Hatano, and X. Hu, Phys. Rev. B **72**, 174514 (2005), and references therein.
¹¹ L. N. Bulaevskii and A. E. Koshelev, Phys. Rev. Lett. **97**, 267001 (2006), and references therein.
¹² R. Kleiner, Phys. Rev. B **50**, 6919 (1994).
¹³ V. M. Krasnov, N. Mros, A. Yurgens, and D. Winkler, Phys. Rev. B **59**, 8463 (1999).
¹⁴ S. Ooi, T. Mochiku, and K. Hirata, Phys. Rev. Lett. **89**, 247002 (2002).
¹⁵ M. Machida, Phys. Rev. Lett. **90**, 037001 (2003).
¹⁶ L. N. Bulaevskii, M. Maley, H. Safar, and D. Dominguez, Phys. Rev. B **53**, 6634 (1996).
¹⁷ J. I. Gorina, G. A. Kaljuzhnaia, V. I. Ktitorov, V. P. Martovitsky, V. V. Rodin, V. A. Stepanov, and S. I. Vedenev, Solid State Commun. **91**, 615 (1994).
¹⁸ V. P. Martovitsky, J. I. Gorina, and G. Kaljuzhnaia, Solid State Commun. **96**, 893 (1995).
¹⁹ S. I. Vedenev and D. K. Maude, Phys. Rev. B **70**, 184524 (2004).
²⁰ The contacts on both ab surfaces of the sample also allows us to measure ρ_c which is required to determine the transport anisotropy.
²¹ S. I. Vedenev, C. Proust, V. P. Mineev, M. Nardone, and G. L. J. A. Rikken, Phys. Rev. B **73**, 014528 (2006).
²² X. Hu and M. Tachiki, Phys. Rev. B **70**, 064506 (2004).
²³ Qing-Hu Chen and X. Hu, Phys. Rev. B **75**, 064504 (2007).
²⁴ G. Kotliar and C. M. Varma, Phys. Rev. Lett. **77**, 2296 (1996).
²⁵ A. Schilling, R. Jin, J. D. Guo, and H. R. Ott, Phys. Rev. Lett. **71**, 1899 (1993).
²⁶ S. Luo, G. Yang, and C. E. Gough, Phys. Rev. B **51**, 6655 (1995).
²⁷ A. Morello, A. G. M. Jansen, R. S. Gonnelli, and S. I. Vedenev, Phys. Rev. B **61**, 9113 (2000).
²⁸ A. K. Pradhan, S. J. Hazell, J. W. Hodby, C. Chen, and B. M. Wanklyn, Solid State Commun. **82**, 685 (1992).
²⁹ Y. Wang, S. Ono, Y. Onose, G. Gu, Y. Ando, Y. Tokura, S. Uchida, and N. P. Ong, Science **86**, 299 (2003).
³⁰ V. Sandu, E. Cimpoeasu, T. Katuwal, C. C. Almasan, Shi Li, and M. B. Maple, Phys. Rev. Lett. **93**, 177005 (2004).
³¹ S. S. Maslov and V. L. Pokrovsky, JETP Lett **53**, 636 (1991).
³² O. K. C. Tsui, N. P. Ong, and J. B. Peterson, Phys. Rev. Lett. **76**, 819 (1996).
³³ I. Kakeya, T. Wada, R. Nakamura, and K. Kadowaki, Phys. Rev. B **72**, 014540 (2005).
³⁴ A. E. Koshelev and I. Aranson, Phys. Rev. B **64**, 174508 (2001), and references therein.
³⁵ A. E. Koshelev, Phys. Rev. B **66**, 224514 (2002).
³⁶ S. N. Gordeev, A. A. Zhukov, P. A. J. de Groot, A. G. M. Jansen, R. Gagnon, and L. Taillefer, Phys. Rev. Lett **85**, 4594 (2000).
³⁷ K. C. Woo, K. E. Gray, R. T. Kampwirth, J. H. Kang, S. J. Stein, R. East, and D. M. McKay, Phys. Rev. Lett. **63**, 1877 (1989).